

Analysis of multi-constellation GNSS PPP solutions under phase scintillations at high latitudes

Original

Analysis of multi-constellation GNSS PPP solutions under phase scintillations at high latitudes / Dabove, P.; Linty, N.; Dosis, F.. - In: APPLIED GEOMATICS. - ISSN 1866-9298. - STAMPA. - (2019). [10.1007/s12518-019-00269-4]

Availability:

This version is available at: 11583/2737432 since: 2019-07-01T17:00:00Z

Publisher:

Springer Verlag

Published

DOI:10.1007/s12518-019-00269-4

Terms of use:

This article is made available under terms and conditions as specified in the corresponding bibliographic description in the repository

Publisher copyright

Springer postprint/Author's Accepted Manuscript

This version of the article has been accepted for publication, after peer review (when applicable) and is subject to Springer Nature's AM terms of use, but is not the Version of Record and does not reflect post-acceptance improvements, or any corrections. The Version of Record is available online at: <http://dx.doi.org/10.1007/s12518-019-00269-4>

(Article begins on next page)

Analysis of multi-constellation GNSS PPP solutions under phase scintillations at high latitudes

Paolo Dabove · Nicola Linty ·
Fabio Dovis

Received: date / Accepted: date

Abstract In the past few years, the rapid evolution of multi-constellation navigation satellite systems boosted the development of many scientific and engineering applications. More than 100 satellites will be available in a few years, when all the four global constellations (GPS, GLONASS, Galileo and Beidou) will be fully deployed. This high number of visible satellites has improved the performance of Precise Point Positioning (PPP) techniques both in terms of accuracy and of session length, especially easing the modeling of ionospheric biases. However, in the presence of severe environmental and atmospheric conditions, the performance of PPP considerably deteriorates. It is the case of high latitude scenarios, where the satellites coverage is limited, the satellites geometry is poor and ionospheric scintillation are frequent. This paper analyzes the quality of PPP solutions in terms of accuracy and convergence time, for a GNSS station in Antarctica. Single and multi-constellation results are compared, proving the benefits of the availability of a higher number of satellites as well as the improved robustness to the presence of moderate and strong phase scintillations. The use of PPP multi-constellation at high-latitudes is indeed essential to guarantee high accuracy, and to obtain a low convergence time, of the order of tens of minutes.

Keywords GNSS · Ionospheric scintillations · Multi-constellation · PPP

1 Introduction

Precise point positioning (PPP) is one of the most used Global Navigation Satellite System (GNSS) high quality positioning techniques, offering to single receivers

P. Dabove

Department of Environment, Land and Infrastructure Engineering (DIATI), Politecnico di Torino, Corso Duca degli Abruzzi 24, 10129 Turin, Italy

Tel.: +39-011-0907662

E-mail: paolo.dabove@polito.it

N. Linty · F. Dovis

Department of Electronics and Telecommunications (DET), Politecnico di Torino, Corso Duca degli Abruzzi 24, 10129 Turin, Italy.

E-mail: nicola.linty@polito.it, fabio.dovis@polito.it

decimetre-level positioning employing models and corrections generated by global reference stations, with no need of base stations. The main difference with respect to the classic double difference Real Time Kinematic (RTK) approach is that PPP provides an absolute positioning, rather than the location relative to the RTK reference station [1]. However, the two main limitations of PPP are the long convergence time, of the order of tens of minutes, while for RTK techniques a couple of minutes are enough [2], and the difficulty to accurately model atmospheric delay and ionospheric scintillations [3].

In particular, despite all the efforts for improving the quality of GNSS position estimation, ionosphere remains the major source of errors in GNSS positioning [4]. While the first order ionospheric delay can be compensated by means of double frequency measurements, ionospheric irregularities and gradients are still hard to be modelled and mitigated. For instance, ionospheric scintillations can severely impact the quality of the received signal and, in turn, the accuracy and reliability of the positioning estimate [5]. The combined use of precise satellite position and clock data, and of a double frequency receiver which removes the first order effect of the ionosphere, increases the accuracy from a couple of decimeters to few centimeters [6]. Precise orbit and clock data [7] can be obtained from a relatively sparse network of reference stations, with inter-station distances of about thousands of kilometers; networks of reference stations are defined sparse when the maximum inter-station distance is larger than 200 km [8].

Given this, PPP is today a very interesting alternative to RTK, where dense RTK networks are not available, e.g. in low-density urban areas and in remote locations. Many PPP online services and offline softwares for post-processing are available [9]. With the advent of cost-effective, accurate, RTK positioning provided by an increasing number of Continuously Operating Reference Station (CORS) networks around the world, there is a strong interest to study real-time [10] or near real-time PPP solutions [11]. The interest in the PPP technique has grown in recent years, being particularly stimulated by the increase in the total number of satellites available from different constellations [12], [13]: in October 2011 GLONASS has been declared fully operational, while Galileo started its initial service in December 2016 and it will reach a full operational capability by 2020. Such a large number of satellites expands the possibility to perform accurate positioning, increasing the redundancy of the available signals [14].

This paper addresses the analysis of the accuracy of PPP algorithms at high latitudes and in the presence of ionospheric phase scintillations. Furthermore, it analyzes the impact of this kind of disturbances on multi-constellation solutions. It is well known that dual-constellation and triple constellation receivers provide more accurate solutions; however, there are few studies regarding the benefits of GLONASS constellation [15] but no studies about the benefits of GLONASS and Galileo constellations for high-latitude PPP and in the presence of phase scintillations. Finally, besides the usual statistical considerations on the accuracy of the positioning solutions, this paper also considers the convergence time as a figure of merit for assessing the performance of PPP.

After an introduction on GNSS signals, ionospheric scintillations, and PPP, a description of the data collection site and of the data collected is given in Section 3. Section 4 provides results related to single events, and overall statistical considerations. Conclusions and remarks are outlined in Section 5

2 Signal and system model

2.1 GNSS signals and scintillation

Ionospheric scintillations are due to irregular electron density concentrations, small-scale spatial irregularities, geo-magnetic storms and strong space weather events. A summary of models of ionospheric scintillations can be found in [16].

As GNSS electromagnetic radio signals pass through ionosphere, they are affected by diffraction and refraction phenomena, leading to rapid fluctuations in their intensity and phase. In the particular case of polar ionosphere, solar energetic particles driven by the cusps of the geomagnetic field mainly induce phase scintillations.

The time-varying GNSS signal at the receiver input, S , in the presence of scintillations, can be modelled [17] as:

$$S = Ae^{j\phi} = S_0\tilde{S} = A_0\tilde{A}e^{j(\phi_0+\tilde{\phi})} . \quad (1)$$

$S_0 = A_0e^{j\phi_0}$ is the nominal received GNSS signal in the absence of scintillation, while $\tilde{S} = \tilde{A}e^{j\tilde{\phi}}$ is the contribution of scintillation. The scintillation signal \tilde{S} can be modelled as a Nakagami-m distribution for the intensity, and as a Gaussian distribution with zero mean and standard deviation $\sigma_{\tilde{\phi}}$ for the phase [17].

S is the contribution of one single satellite, in the absence of noise. The overall received signal, as the contribution of L different satellite-receiver links (including different constellations and different bandwidths) and of thermal noise η is:

$$R = \sum_L S + \eta . \quad (2)$$

Scintillations might lead to performance degradation, losses of lock and even complete receiver outage. Strong signal fading induced by amplitude scintillation, modelled by \tilde{A} , can decrease the C/N_0 and reduce the sensitivity of the receiver. Similarly, fast changes of the phase, induced by $\tilde{\phi}$, alter the capability of the tracking loops to follow the apparent signal dynamics, potentially leading to cycle slips and losses of lock. The tracking error variance at the output of the Phase Lock Loop (PLL) can be computed as

$$\sigma_{\phi_e}^2 = \sigma_{\phi_\eta}^2 + \sigma_{\tilde{\phi}}^2 , \quad (3)$$

where $\sigma_{\phi_\eta}^2$ is the jitter contribution in the absence of scintillation, due to thermal noise and oscillators noise, while $\sigma_{\tilde{\phi}}^2$ corresponds to the jitter contribution due to phase scintillation [18].

In the particular case of PPP, scintillation can affect cycle slip detection and correction procedures, leading to significant degradation of point positioning results [19] and errors of the order of meters [20]. A jump of one cycle in the L1 carrier corresponds to an error of 48 cm in the iono-free combination used in PPP, thus canceling the added value of PPP. For these reasons, it is important to monitor the occurrence and intensity of such events.

2.2 PPP and multi-constellation receivers

The advantages of multi-constellation processing have been extensively studied. When signals from different constellations are used, the position solution accuracy significantly increases, and, at the same time, the convergence time decreases [21]. When comparing a GPS-GLONASS solution to a GPS-only scenario, the convergence time is reduced from 21.6 to 15.7 minutes in static mode and from 34.4 to 20.0 minutes in kinematic mode [22]. Other works [23] demonstrated that the average convergence time for the GPS-only case is 68, 43, and 93 minutes in the East, North, and Up directions respectively. Adding GLONASS, the convergence time is reduced by 38%, 42%, and 34% respectively.

This is mainly due to the availability of a larger number of satellites and, in turn, of signals, making the positioning algorithm more robust and enabling the possibility to discard low quality measurements. In addition, a better Geometrical Dilution of Precision (GDOP) can be obtained, thus reducing the geometrical contribution to the error variance.

Nevertheless, such results are valid as long as no atmospheric disturbances occur. In the presence of ionospheric scintillations, the convergence time drastically increases up to a couple of hours. Several analyses of the impact of scintillation on PPP are present in literature, in particular for what concerns equatorial regions. In different studies it has been proven that scintillations affect the quality of the solution in terms of accuracy [22,23]. The work in [24] investigated the relationship between the rate of change of the Total Electron Content (TEC) and PPP errors. The error in the position estimate can increase by an order of magnitude under disturbed geo-magnetic conditions. Bougard et al. [25] proposed a mitigation strategy, based on the assessment of the phase residual and removal of the satellites affected by scintillation. Zhang et al. [26] proposed a method to avoid unnecessary re-initializations of PPP, thus preventing sudden variations in estimated position and maintaining a centimeter level accuracy. In [19] and [27], PPP and ionospheric-free combination measurements are used to detect scintillation. Concerning multi-constellation, there are limited works dealing with ionospheric scintillations. Cai et Gao proposed a combined GPS-GLONASS PPP model and demonstrated the benefits of dual-constellation PPP, showing that while the convergence time can be significantly reduced, the accuracy is not improved, as long as GPS satellites visibility is good [28]; however, no results concerning scintillation were presented. Li et al. have developed a four-system positioning model and showed that multi-GNSS brings to precise positioning a significant improvement of satellite visibility, spatial geometry, dilution of precision, convergence, accuracy, continuity and reliability [29]. Nevertheless, despite they claim that in the presence of ionospheric scintillations the availability of more satellites is important, they do not provide results on real data. The advantages of adding GLONASS observation to GPS was assessed by Marques et al. [30]. Accuracy improvements of 60% were experienced, when processing multi-constellation data in kinematic PPP mode, under strong equatorial scintillation. Similar results were shown in [31], where improvements in positioning accuracy of the order to 70% in height component are presented, when using GPS and GLONASS compared with PPP using only GPS data, under equatorial scintillations. Most of these works indeed focus on equatorial regions and on amplitude scintillation, while minor attention was given to high latitude regions [24,32]. In particular, the use of Galileo sig-

nals in Antarctica for scintillation observation is still almost unexplored, due to the limited availability of Galileo-ready professional receivers operational in the region [33].

3 Data and test-site description

Data used in this study were collected in 2016 at the South African Antarctica research station SANAE IV, as part of the DemoGRAPE project [34]. The geographic coordinates are $71^{\circ} 40' 22''$ S, $2^{\circ} 50' 26''$ W, while the geomagnetic latitude at time of the data collection was $66^{\circ} 45'$ S. A geodetic GNSS antenna and receiver were installed in January 2016 for scintillation monitoring purposes. The receiver is a *Septentrio PolaRxS PRO* multi-constellation and multi-frequency receiver, able to track signals from GPS, GLONASS and Galileo. The receiver was configured to store RINEX and ismr files, the latter containing also the scintillation indices [35,36].

The reference antenna coordinates are obtained processing 7 different datasets of 24 hours each, with a sampling rate of 1 s, using the Bernese GNSS Software Version 5.2, with an elevation angle cutoff of 7° and considering a double difference approach and the ionosphere-free linear combination [37]. The coordinates adjustment is made considering 14 GNSS permanent stations, depicted in red in Fig. 1, and a weighted least-squares algorithm. Coordinate constraints are applied at the reference sites with standard deviation of 1 mm and 2 mm for horizontal and vertical components, respectively. Ambiguities are resolved in a baseline-by-baseline mode using the Code-Based strategy for all baselines [37]. These solutions were compared with the results of the AUSPOS Online GPS Processing Service version 2.2, used as benchmark in the analysis of the PPP accuracy.

Table 1 reports a summary of the days considered in this work. During these time slots, significant phase scintillation events with a duration of at least three hours were detected by the Septentrio receiver. Furthermore, data of October 11 were included as a representative example of a scintillation-free scenario: no details about the other dataset of this kind of scenario are shown because the performances and results are comparable in terms of accuracy.

Phase scintillations are evaluated by means of the Phi60 index, corresponding to the standard deviation of the detrended phase measurements over an interval of 60 seconds. Values of Phi60 between 0.3 and 0.5 rad correspond to moderate scintillation, while strong scintillation is present when Phi60 exceeds 0.5 rad.

Two different examples of scintillation activities are considered, representative of a moderate and a strong scintillation scenario respectively:

1. Fig. 2 reports a linear plot of the values of the phase scintillation index for GPS L1 C/A signals along 24 hours on February 8, 2016. Moderate scintillation activity can be identified from 00:00 to 07.30 UTC.
2. Fig. 3 reports the same index on May 9, 2016, with a Phi60 up to about 1.4 rad. Strong scintillation is present approximately in the same time range.

Data are filtered at an elevation mask of 30° , to reduce the occurrence of high Phi60 values due to multipath reflections on low elevation satellites rather than to ionospheric disturbances.

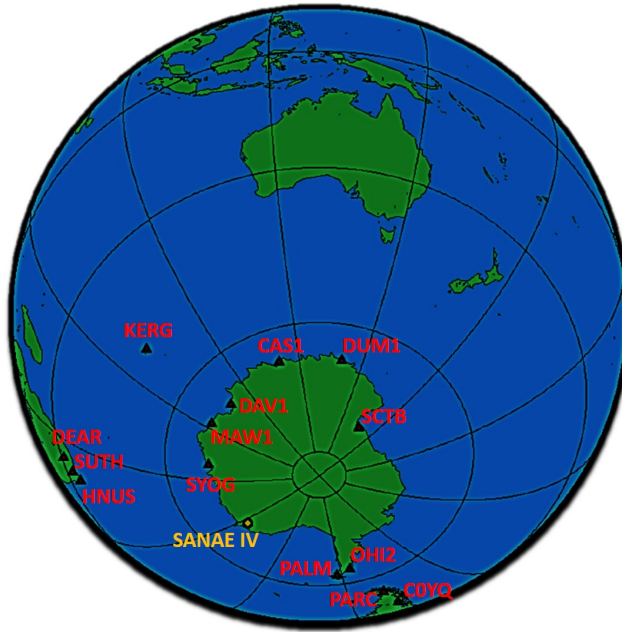


Fig. 1 GNSS permanent master stations, in red, used for estimating the reference position of the SANA IV station, in yellow.

Table 1 Summary of data used for PPP analysis, including the time range in which scintillation has been detected ($\text{Phi60} > 0.3$ rad and elevation $> 30^\circ$), the number of GPS, GLONASS and Galileo satellites affected over the total number of satellites in view and the maximum Phi60 values.

| Date (2016) | Start and end (UTC) of scintillation event | Satellites affected | maximum Phi60 (rad) |
|----------------|-----------------------------------------------|------------------------|---------------------------------|
| January 20 | 16:00 – 22:00 | 16 / 69 | 0.8 |
| February 3 | 00:00 – 06:00 | 18 / 59 | 1.1 |
| February 8 | 00:00 – 07:30 | 21 / 60 | 1.1 |
| February 18 | 00:00 – 07:00 | 22 / 59 | 1.0 |
| April 2 | 21:00 – 24:00 | 18 / 63 | 1.4 |
| April 13 | 00:00 – 08:00 | 34 / 63 | 1.1 |
| May 9 | 00:00 – 06:00 | 23 / 63 | 1.4 |
| June 6 | 00:00 – 06:30 | 21 / 64 | 1.4 |
| October 13 | 11:00 – 21:00 | 31 / 66 | 1.4 |
| January 13 | no scintillation | 0 | 0.1 |
| February 28 | no scintillation | 0 | 0.1 |
| April 25 | no scintillation | 0 | 0.1 |
| May 18 | no scintillation | 0 | 0.1 |
| October 11 | no scintillation | 0 | 0.1 |
| October 16 | no scintillation | 0 | 0.1 |
| October 25 | no scintillation | 0 | 0.1 |

The GNSS satellites coverage is reduced at the poles, compared to low and medium latitudes: Fig. 4 reports the skyplot over 24 hours from the SANA IV station. No satellites at high elevation are present, in particular towards the

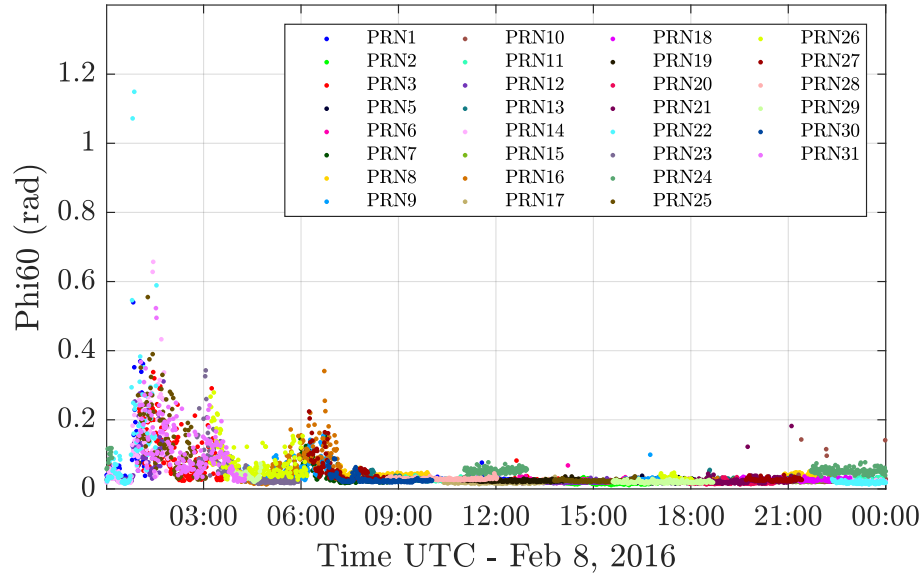


Fig. 2 Phase scintillation index for GPS L1 C/A satellites (elevation mask 30°) in case of moderate scintillation.

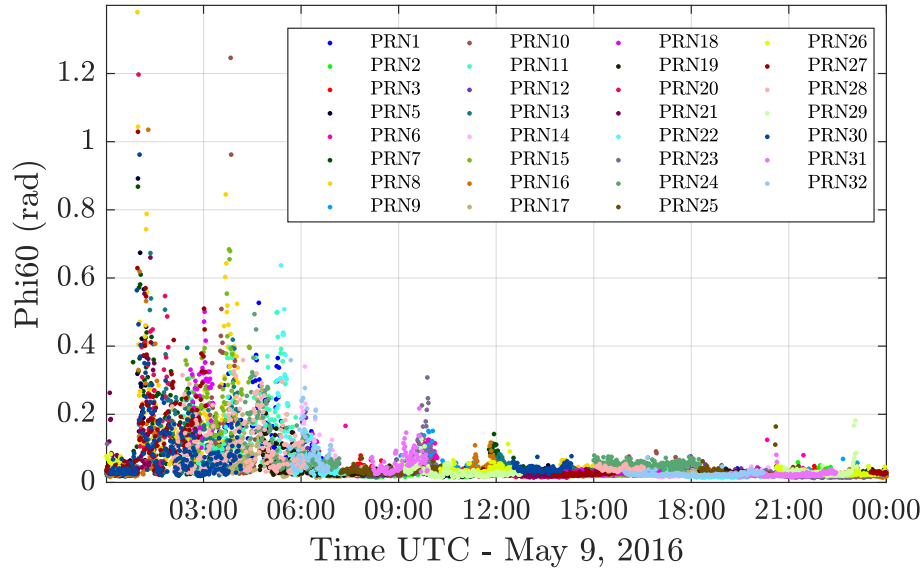


Fig. 3 Phase scintillation index for GPS L1 C/A satellites (elevation mask 30°) in case of strong scintillation.

South direction. GPS satellites have a reduced coverage of this area, while Galileo and GLONASS satellites reach a higher elevation in the sky. For this reason, the contribution of the latter constellations for PPP is even more relevant in Antarctica.

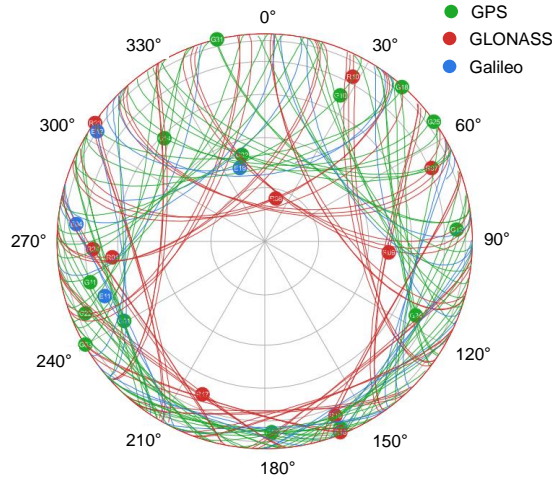


Fig. 4 Skyplot of GPS, GLONASS and Galileo satellites over 24 hours from SANAE IV station.

4 Analysis of PPP accuracy and convergence time

In this section, an analysis of accuracy and convergence time of PPP solutions is made, by processing different datasets collected at SANAE IV. Results are obtained exploiting a modified version of the RTKLIB software [38], considering a kinematic PPP approach based on a smoother combined (forward and backward) filter solution, a cutoff angle of 10° , final CODE (Center for Orbit Determination in Europe) products for ephemeris and clocks, considering also earth rotation parameters (ERP) and differential code biases (DCB). Both single and multiple constellation combinations are considered, in three different test cases: GPS-only, GPS/GLONASS, and GPS/GLONASS/Galileo. The number of visible GPS satellites varies from 11 to 13, from 18 to 24 and from 22 to 29 in case of GPS-only, GPS/GLONASS and GPS/GLONASS/Galileo, respectively. About the geometric distribution of visible satellites, the maximum values of GDOP indexes are 2.7 for the GPS-only case, 2.3 for GPS/GLONASS and 1.8 for GPS/GLONASS/Galileo. Furthermore, the particular case of the presence of ionospheric scintillations is analyzed in details.

The Root Mean Square (RMS) error is defined as the square root of the arithmetic mean of the squares of the values evaluated as differences between estimated values with respect to the reference ones. The convergence time is defined as the interval from the first epoch processed to the epoch the horizontal component bias of which is lower than 10 cm, and the height component bias is lower than 15 cm, provided that the average deviation of the next 20 consecutive epochs also satisfies these requirements.

Table 2 RMS statistics of PPP *kinematic* solutions for three different constellation combinations in the absence of scintillations.

| | GPS | GPS/GLO | GPS/GLO/GAL |
|-----------|-------|---------|-------------|
| East (m) | 0.064 | 0.015 | 0.008 |
| North (m) | 0.032 | 0.024 | 0.011 |
| Up (m) | 0.045 | 0.031 | 0.028 |

Table 3 Convergence time for PPP *kinematic* solutions for three different constellation combinations in the absence of scintillations. The improvements of multi-constellation results with respect to the GPS-only case are shown in brackets.

| | GPS | GPS/GLO | GPS/GLO/GAL |
|-----------------|-----|-----------|-------------|
| East (minutes) | 21 | 13 (−38%) | 10 (−53%) |
| North (minutes) | 18 | 10 (−42%) | 9 (−48%) |
| Up (minutes) | 34 | 22 (−34%) | 21 (−37%) |

4.1 Scintillation-free scenario

In order to determine a benchmark, a scintillation free scenario is considered. Many data collected in different days without any scintillation activity ($\text{Phi60} \leq 0.1$ on all visible satellites along the whole observation window) are considered and processed, as reported in the second part of Table 1: in all cases, the obtained results are comparable to each others and there are no substantial differences. The data collected on October 11, 2016, are shown as representative as scintillation-free scenario.

Table 2 reports the RMS statistics for the three test cases, considering 24 hours of observations, and a sampling rate of 1 s. As expected, the positioning performance improves when multiple constellations are considered. Moreover, if we add the observations obtained by Galileo satellites, the performance further improves if compared to the GPS/GLONASS solution. The RMS values for East and North components have dropped by half, while the Up component estimation slightly improves.

As expected, the convergence time of the PPP solutions changes as a function of the number of constellations considered.

The results are reported in Table 3. The convergence time for the GPS-only case is equal to 21, 18, and 34 minutes in the East, North, and Up directions, respectively. Adding GLONASS, the convergence time is reduced by 38%, 42%, and 34% for the three components. If the Galileo constellations is also considered, the improvement reaches 53%, 48%, and 37%. As also discussed in [23], the East coordinate component needs longer time to converge than the North coordinate component, due to the satellites constellation geometry.

4.2 Moderate and high phase scintillations

Considering the same GNSS station, nine different days characterized by moderate and high ionospheric scintillation activity have been taken into account, as reported in Table 1. Since the behavior of the results is the same regardless of

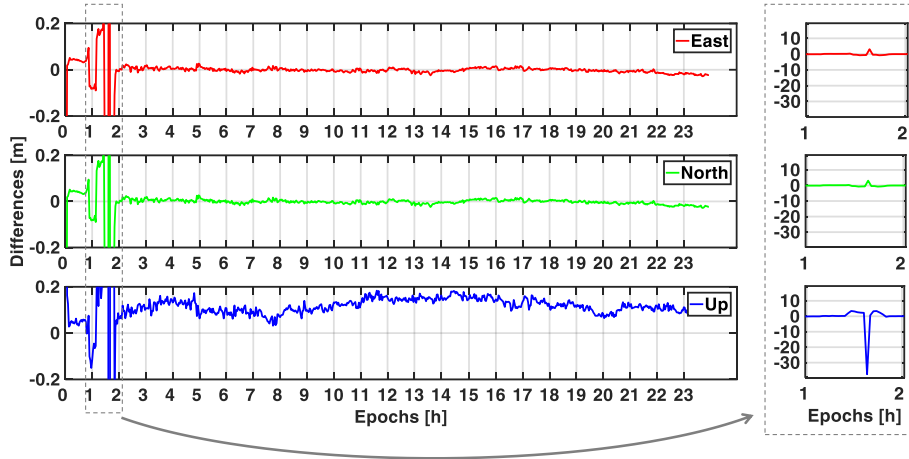


Fig. 5 Differences of East, North and Up components between PPP *kinematic* solutions with respect to the reference one, obtained considering the Bernese solution, following a double difference approach coupled with the iono-free linear combination, on February 8, 2016.

Table 4 RMS statistics of PPP *kinematic* solutions for three different constellation combinations in the presence of moderate scintillation activity.

| | GPS | GPS/GLO | GPS/GLO/GAL |
|-----------|-------|---------|-------------|
| East (m) | 0.170 | 0.120 | 0.118 |
| North (m) | 0.096 | 0.074 | 0.069 |
| Up (m) | 0.268 | 0.194 | 0.179 |

the ionospheric scintillation events, only the results of February 8, 2016 and May 9, 2016 are shown as example of moderate and high phase scintillation events, respectively. In the first case, the scintillation activity is concentrated from 00:00 to 07:30 UTC time, as shown in Fig. 2, with a peak between 01:00 and 02:00 UTC. In the second case, phase scintillation is recorded from 00:00 to 09:00 UTC, with strong peaks around 01:00, as shown in Fig. 3.

Fig. 5 shows the East, North and Up PPP error over 24 hours for data of February 8. The impact of phase scintillations on the results is evident. In particular, the error on the Up component reaches 40 m. Furthermore, the fact that scintillations are concentrated at the beginning of the measurement session further affects the initial convergence time. This corresponds to the worst scenario.

Table 4 summarizes the RMS of all the components computed processing a 24-hours observation file of the moderate scintillation activity scenario, for the three constellation combinations considered. As for the GPS-only configuration, the RMS values are about three times higher in presence of scintillation. Adding one or more constellations, the results improve, even though the benefits are less remarkable than in the scintillation-free case.

Comparing Table 4 and Table 5, it is evident how the scintillation effects impact on the RMS values of PPP results. The benefit of the use of GPS/GLONASS constellations against the GPS-only is not only for estimating the Up component: in this case, the improvement is about 28% and 44% when moderate and high

Table 5 RMS statistics of PPP *kinematic* solutions for three different constellation combinations in the presence of high scintillation activity.

| | GPS | GPS/GLO | GPS/GLO/GAL |
|-----------|-------|---------|-------------|
| East (m) | 0.221 | 0.132 | 0.116 |
| North (m) | 0.206 | 0.141 | 0.117 |
| Up (m) | 0.384 | 0.216 | 0.188 |

Table 6 Convergence time for PPP *kinematic* solutions for three different constellation combinations in the presence of moderate scintillations.

| | GPS | GPS/GLO | GPS/GLO/GAL |
|-----------------|-----|-----------|-------------|
| East (minutes) | 65 | 43 (−34%) | 38 (−42%) |
| North (minutes) | 38 | 21 (−45%) | 20 (−47%) |
| Up (minutes) | 95 | 49 (−48%) | 41 (−57%) |

scintillation activities are considered, respectively. However, this advantage is also visible if the planimetric components are considered: the percentage is about 42% and 23% for East and North components in case of medium scintillation while 40% and 32% in case of high activity. The contribution of the Galileo constellation in this case is not so strong, due to the reduced number of visible satellites during the acquisition phase (2016). Considering the GPS/GLONASS/Galileo results compared to the GPS/GLONASS ones, the improvements are about 2%, 7% and 8% considering medium activity and 12%, 17% and 13% in presence of high scintillation. The benefits are more visible and important if the GPS/GLONASS/Galileo results are compared to the GPS-only ones: in this case the improvements are about 31%, 28% and 33% considering a medium activity, while 47%, 43% and 51% in presence of high scintillation.

As far as the convergence time is concerned, analyzing the moderate scenario and considering the GPS-only constellation, the solution converges after 65, 38 and 95 minutes in the East, North and Up components respectively. If the GPS/GLONASS configuration is considered, the convergence time decreases down to 43, 21 and 49 minutes, as summarized in Table 6. Moreover, if a third constellation is considered the solution converges more quickly, in about 40 minutes for all components. In case of high scintillation activity, the results are slightly worse, as shown in Table 7: considering the GPS-only constellation, the solution converges after 74, 53 and 96 minutes in the East, North and Up components respectively, while adding the GLONASS constellation to the GPS one, the results are better: in this case, the solution converges in 63, 48 and 62 minutes. Adding the Galileo constellation, there are no improvements in terms of convergence time: in this last case the solution converges in 53, 41 and 52 minutes, with an improvement of about 25 % for East and North components and about 46 % for the Up respect to the GPS-only solution. This means that it is possible to reach a level of accuracy of few centimeters in less than 1 hour, if multi-constellation solutions are considered, even in presence of high ionospheric scintillation activity.

Table 7 Convergence time for PPP *kinematic* solutions for three different constellation combinations in the presence of high scintillations.

| | GPS | GPS/GLO | GPS/GLO/GAL |
|-----------------|-----|-----------|-------------|
| East (minutes) | 71 | 63 (−11%) | 53 (−25%) |
| North (minutes) | 53 | 48 (−9%) | 41 (−23%) |
| Up (minutes) | 96 | 62 (−35%) | 52 (−46%) |

5 Conclusion

Despite being one of the most used GNSS positioning techniques, PPP is limited by the long convergence time and the accurate modeling of atmospheric delays, especially under disturbed ionospheric conditions. This effect is magnified at higher latitudes, where the satellites visibility is limited and ionospheric scintillations are more frequent and intense: such events impact the quality of the GNSS positioning solutions in terms of accuracy and convergence time. This paper has demonstrated the usefulness of a multi-constellation receiver for PPP in the presence of intense ionospheric activity, for sites located at high latitude. The benefits of multi-constellation solutions are not only related to the improvement of accuracy but also to the reduction convergence time. Under quiet ionospheric conditions, the multi-constellation approach allows to reduce the convergence time by about 40% for all components and the RMS values are in average two times lower than the GPS-only solutions. In the presence of moderate and high scintillation activity, the use of GLONASS and Galileo satellites reduces the convergence time, enabling significantly faster PPP solutions. These results confirm that, when performing PPP measurements in polar regions, it is important to verify the presence of ionospheric scintillation, as they afflict the quality of the solution, especially if such events are concentrated at the beginning of the measurement session.

Acknowledgment

The authors would like to thank Pierre Cilliers, on behalf of SANSA, and Lucilla Alfonsi, on behalf of INGV. Data used in this study are part of the DemoGRAPE project (funded by PNRA, contract 2013/C3.01).

References

1. L. Banyai, A.-M. S. Mohamed, E. Szűcs, N. Aboaly, A. Mousa, and H. A. Khalil, “The relationship between global plate motion and intra-plate deformation analysis of Cairo network: case study with simulated data,” *Arabian Journal of Geosciences*, vol. 9, no. 1, p. 76, Dec 2015.
2. P. Dabove, A. M. Manzano, and C. Taglioretti, “GNSS network products for post-processing positioning: limitations and peculiarities,” *Applied Geomatics*, vol. 6, no. 1, pp. 27–36, 2014.
3. J. Zumberge, M. Heflin, D. Jefferson, M. Watkins, and F. H. Webb, “Precise point positioning for the efficient and robust analysis of GPS data from large networks,” *Journal of Geophysical Research: Solid Earth*, vol. 102, no. B3, pp. 5005–5017, 1997.
4. J. Lee, Y. J. Morton, J. Lee, H.-S. Moon, and J. Seo, “Monitoring and mitigation of ionospheric anomalies for GNSS-based safety critical systems: A review of up-to-date signal processing techniques,” *IEEE Signal Processing Magazine*, vol. 34, no. 5, pp. 96–110, 2017.

5. P. M. Kintner, B. M. Ledvina, and E. R. de Paula, "GPS and ionospheric scintillations," *SPACE WEATHER*, vol. 5, no. 9, 2007.
6. J. Kouba and P. Héroux, "Precise point positioning using IGS orbit and clock products," *GPS Solutions*, vol. 5, no. 2, pp. 12–28, Oct 2001.
7. T. Grinter and C. Roberts, "Precise point positioning: Where are we now?," *International Global Navigation Satellite Systems Society IGSS Symposium*, 2011.
8. A.R. Snay, and T. Soler, "Continuously Operating Reference Station (CORS): History, Applications, and Future Enhancements" *Journal of Surveying Engineering*, vol. 134, no. 4, pp. 95–104, 2008.
9. P. Dabove, M. Piras, and K. N. Jonah, "Statistical comparison of PPP solution obtained by online post-processing services," in *IEEE/ION PLANS*, pp. 137–143, 2016.
10. J. Geng and C. Shi, "Rapid initialization of real-time PPP by resolving undifferenced GPS and GLONASS ambiguities simultaneously," *Journal of Geodesy*, vol. 91, no. 4, pp. 361–374, 2017.
11. X. Tang, G. W. Roberts, X. Li, and C. M. Hancock, "Real-time kinematic PPP GPS for structure monitoring applied on the Severn suspension bridge, UK," *Advances in Space Research*, 2017.
12. R. Romero, N. Linty, C. Cristodaro, F. Dovis, and L. Alfonsi, "On the use and performance of new Galileo signals for ionospheric scintillation monitoring over Antarctica," *2017 International Technical Meeting of The Institute of Navigation*, pp. 989–997, 2017.
13. B. Federici, D. Giacomelli, D. Sguerso, A. Vitti, P. Zatelli, "A web processing service for GNSS realistic planning," *Applied Geomatics*, vol. 5, no. 1, pp. 45–57, 2013.
14. J. Tegeedor, O. Øvstedal, and E. Vigen, "Precise orbit determination and point positioning using GPS, BeiDou, GLONASS and Galileo," *Journal of geodetic science*, vol. 4, no. 1, 2014.
15. J.M. Juan, J. Sanz , G. González-Casado , A. Rovira-Garcia , A. Camps , J. Riba , J. Barbosa , E. Blanch , D. Altadill , R. Orus, "Feasibility of precise navigation in high and low latitude regions under scintillation conditions," *Journal of Space Weather Space Climate*, vol. 8, no. A05, pp. 1–11, 2018.
16. S. Priyadarshi, "A review of ionospheric scintillation models," *Surveys in geophysics*, vol. 36, no. 2, pp. 295–324, 2015.
17. C. Hegarty, M. B. El-Arini, T. Kim and S. Ericson, "Scintillation modeling for GPS-wide area augmentation system receivers," *Radio Science*, vol. 36, no. 5, pp. 1221–1231, 2001.
18. M. Knight, and A. Finn, "The effects of ionospheric scintillations on GPS," *ION GPS-98*, pp. 673–685, 1998.
19. B. Moreno, S. Radicella, M. De Lacy, M. Herraiz, and G. Rodriguez-Caderot, "On the effects of the ionospheric disturbances on precise point positioning at equatorial latitudes," *GPS solutions*, vol. 15, no. 4, pp. 381–390, 2011.
20. V. Sreeja, M. Aquino, K. Jong, and H. Visser, "Effect of the 24 september 2011 solar radio burst on precise point positioning service," *Space Weather*, vol. 12, no. 3, pp. 143–147, 2014.
21. X. Ren, S. Choy, K. Harima, and X. Zhang, "Multi-constellation GNSS precise point positioning using GPS, GLONASS and BeiDou in Australia," in *International Global Navigation Satellite Systems (IGNSS) Symposium*, pp.1–13, 2015.
22. P. Li and X. Zhang, "Integrating GPS and GLONASS to accelerate convergence and initialization times of precise point positioning," *GPS Solutions*, vol. 18, no. 3, pp. 461–471, Jul 2014.
23. C. Cai, Y. Gong, Y. Gao, and C. Kuang, "An approach to speed up single-frequency PPP convergence with quad-constellation GNSS and GIM," *Sensors*, vol. 17, no. 6, p. 1302, 2017.
24. K. S. Jacobsen and M. Dähnn, "Statistics of ionospheric disturbances and their correlation with GNSS positioning errors at high latitudes," *Journal of Space Weather and Space Climate*, vol. 4, p. A27, 2014.
25. B. Bougard, A. Simsky, J.-M. Sleewaegen, J. Park, M. Aquino, L. Spogli, V. Romano, M. Mendona, and J. F. Galera Monico, "CALIBRA: Mitigating the impact of ionospheric scintillation on precise point positioning in Brazil," *7th GNSS Vulnerabilities and Solutions Conference*, 2013.
26. X. Zhang, F. Guo, and P. Zhou, "Improved precise point positioning in the presence of ionospheric scintillation," *GPS Solutions*, vol. 18, no. 1, pp. 51–60, 2014.
27. J. Juan, A. Aragon-Angel, J. Sanz, G. González-Casado, and A. Rovira-Garcia, "A method for scintillation characterization using geodetic receivers operating at 1 Hz," *Journal of Geodesy*, pp. 1–15, 2017.

28. C. Cai, and Y. Gao, "Modeling and assessment of combined GPS/GLONASS precise point positioning," *GPS solutions*, vol. 17, no. 2, pp. 223–236, 2013.
29. X. Li, X. Zhang, X. Ren, M. Fritsche, J. Wickert and H. Schuh, "Precise positioning with current multi-constellation Global Navigation Satellite Systems: GPS, GLONASS, Galileo and BeiDou," *Scientific reports*, vol. 5, no. 8328, 2015.
30. H.A. Marques, H.A.S. Marques, M. Aquino, S. Vadakke Veettil and J.F. Galera Monico, "Accuracy assessment of Precise Point Positioning with multi-constellation GNSS data under ionospheric scintillation effects," *Journal of Space Weather Space Climate*, vol. 8, no. A15, pp. 1–14, 2018.
31. H. A. Marques, "PPP Analysis with GPS and Glonass Integration in Periods Under Ionospheric Scintillation Effects," *Abstracts of AGU Fall Meeting 2015*, 2015.
32. R. Ghoddousi-Fard and F. Lahaye, "High latitude ionospheric disturbances: Characterization and effects on GNSS precise point positioning," in *2015 International Association of Institutes of Navigation World Congress (IAIN)*, Oct 2015, pp. 1–6.
33. N. Vancans, M. Mc Cormack, and M. De Proft, "First recording of scintillation on Galileo signals in Antarctica made by Septentrio's PolaRx5," *Septentrio website*, Jul 2017. [Online]. Available: <http://www.septentrio.com/company/news/first-recording-scintillation-galileo-signals-antarctica-made-septentrio's-polarx5>
34. N. Linty, F. Dovic, F., and L. Alfonsi, "Software-defined radio technology for GNSS scintillation analysis: bring Antarctica to the lab", *GPS Solutions*, vol. 22, no. 4, pp.96, 2018.
35. N. Linty, R. Romero, C. Cristodaro, F. Dovic, M. Bavaro, J. T. Curran, J. Fortuny-Guasch, J. Ward, G. Lamprecht, P. Riley, P. Cilliers, E. Correia, and L. Alfonsi, "Ionospheric scintillation threats to GNSS in polar regions: The DemoGRAPE case study in Antarctica," in *2016 European Navigation Conference (ENC)*, May 2016, pp. 1–7.
36. C. Cristodaro, F. Dovic, N. Linty, and R. Romero, "Design of a configurable monitoring station for scintillations by means of a GNSS software radio receiver," *IEEE Geoscience and Remote Sensing Letters*, no. 99, pp. 1–5, 2018.
37. R. Dach, S. Lutz, P. Walser, P. Fridez, "Bernese GNSS Software Version 5.2. User manual," *Astronomical Institute, University of Bern, Bern Open Publishing.*, DOI: 10.7892/boris.72297; ISBN: 978-3-906813-05-9.
38. T. Takasu, "RTKLIB: An open source program package for GNSS positioning," <http://www.rtklib.com>.
39. T. Takasu, "PPP Ambiguity Resolution Implementation in RTKLIB v 2.4.2," *PP-RTK and Open Standards Symposium*, March 12-13, 2012, Frankfurt am Main, Germany.